

Winds from accretion disks driven by the radiation and magnetocentrifugal force.

Daniel Proga

LHEA, GSFC, NASA, Code 662, Greenbelt, MD 20771; proga@sobolev.gsfc.nasa.gov

Received _____; accepted _____

ABSTRACT

We study the two-dimensional, time-dependent hydrodynamics of radiation-driven winds from luminous accretion disks threaded by a strong, large-scale, ordered magnetic field. The radiation force is mediated primarily by spectral lines and is calculated using a generalized multidimensional formulation of the Sobolev approximation. The effects of the magnetic field are approximated by adding into the equation of motion a force that emulates a magnetocentrifugal force. Our approach allows us to calculate disk winds when the magnetic field controls the geometry of the flow, forces the flow to corotate with the disk, or both. In particular, we calculate models where the lines of the poloidal component of the field are straight and inclined to the disk at a fixed angle.

Our numerical calculations show that flows which conserve specific angular velocity have a larger mass loss rate than their counterparts which conserve specific angular momentum. The difference in the mass loss rate between these two types of winds can be several orders of magnitude for low disk luminosities but vanishes for high disk luminosities. Winds which conserve angular velocity have much higher velocities than angular momentum conserving winds. Fixing the wind geometry stabilizes winds which are unsteady when the geometry is derived self-consistently. The inclination angle between the poloidal velocity and the normal to the disk midplane is important. Non-zero inclination angles allow the magnetocentrifugal force to increase the mass loss rate for low luminosities, and increase the wind velocity for all luminosities. The presence of the azimuthal force does not change the mass loss rate when the geometry of the flow is fixed.

Our calculations also show that the radiation force can launch winds from magnetized disks. The line force can be essential in producing magnetohydrodynamical (MHD) winds from disks where the thermal energy is too low to launch winds or where the field lines make an angle of $< 30^\circ$ with respect to the normal to the disk midplane. In the latter case the wind will be less decollimated near its base by the centrifugal force and its collimation far away from the disk can be larger than the collimation of its centrifugally-driven MHD counterpart.

1. Introduction

Accretion disks are believed to lose mass via powerful outflows in many astrophysical environments such as active galactic nuclei (AGN); many types of interacting binary stars, non-magnetic cataclysmic variables (nMCVs), for instance; and young stellar objects (YSOs). Magnetically driven winds from disks are the favored explanation for the outflows in many of these environments. Blandford & Payne 1982 (see also Pelletier & Pudritz 1992) showed that the centrifugal force can drive a wind from the disk if the poloidal component of the magnetic field, \mathbf{B}_p makes an angle of $> 30^\circ$ with respect to the normal to the disk surface. Generally, centrifugally-driven MHD disk winds (magnetocentrifugal winds for short) require the presence of a sufficiently strong, large-scale, ordered magnetic field threading the disk and the poloidal magnetic field to be comparable to the toroidal magnetic field, $|B_\phi/B_p| \lesssim 1$ (e.g., Cannizzo & Pudritz 1988, Pelletier & Pudritz 1992). Additionally, magnetocentrifugal winds require some thermal assistance to flow freely and steadily from the surface of the disk, to pass through a slow magnetosonic surface (e.g., Blandford & Payne 1982).

Many authors have studied magnetocentrifugal winds from a Keplerian disk (e.g., Ouyed & Pudritz 1997, Ustyugova et al. 1999, Krasnopolsky, Li & Blandford 1999, and references therein). These studies are either analytic, looking for stationary, often self-similar solutions or numerical, looking for both stationary and time-dependent solutions. However in numerical simulations of magnetocentrifugal winds, the lower boundary is between the slow magnetosonic surface and the Alfvén surface. This specification requires setting the mass loss rate in advance (e.g., Bogovalov 1997). Simulations of magnetocentrifugal winds considering the whole disk (even regions below the slow magnetosonic surface) and not requiring an *ad hoc* mass loss rate, are only now becoming feasible. This requires, however, an accurate treatment of the radiation and gas pressure effects, among other physical processes.

Thermal expansion and the radiation force have been suggested as other mechanisms that can drive disk winds. These mechanisms can produce powerful winds without the presence of a magnetic field. Winds are likely thermally driven in X-ray-irradiated accretion disks in systems such as X-ray binaries and AGNs (e.g., Begelman, McKee & Shields 1983, Woods et al. 1996). These winds require the gas temperature to be so high that the gas is not gravitationally bound. In such cases, the radiation driving is probably not important because the gas is fully ionized, at least in the hottest regions, and the radiation force is only due to electron scattering. However in the regions where gas is cooler and not fully ionized

the radiation force will be enhanced by spectral lines and play an important role in controlling the dynamics of the flow. In fact Murray et al. (1995) designed a line-driven disk wind model specifically for AGNs.

Radiation-driven disk winds have been extensively modeled (e.g., Pereyra, Kallman & Blondin 1997; Proga, Stone & Drew 1998, hereafter PSD I; Proga 1999; Proga, Stone & Drew 1999, hereafter PSD II). These recent studies showed that radiation pressure due to spectral lines can drive winds from luminous disks. This result has been expected (e.g., Vitello & Shlosman 1988). These studies, in particular those by PSD I, also showed some unexpected results. For example, the flow is unsteady in cases where the disk luminosity dominates the driving radiation field. Despite the complex structure of the unsteady disk wind, the time-averaged mass loss rate and terminal velocity scale with luminosity, as do steady flows obtained where the radiation is dominated by the central object.

To calculate the line force for disk winds, PSD I adopted the method introduced by Castor, Abbott & Klein (1975, hereafter CAK) and further developed by Friend & Abbott (1986), Pauldrach, Puls & Kudritzki (1986) for one-dimensional radial flows within the context of a wind from hot, luminous OB stars. To extend the CAK method to model multi-dimensional disk winds, it is necessary to accommodate the effects of the three-dimensional velocity field and the direction-dependent intensity. Owocki, Cranmer & Gayley (1996) showed that these effects can lead to qualitatively different results compared to those obtained from a one-dimensional treatment in the case of a rapidly rotating star. The most difficult aspect of calculating the line force due to a disk is in the evaluation of the integral involving the velocity gradient tensor over the entire solid angle occupied by the radiating surface. PSD I used an angle-adaptive quadrature to ensure an accurate result. However, computational limitations required that they simplified the integrand, retaining only the dominant terms in the velocity gradient tensor.

PSD II generalized the PSD I method and introduced a new quadrature that avoids any simplification of the integrand. This allowed them to evaluate the radiation force for completely arbitrary velocity fields within the context of the CAK formalism. They applied this method to recalculate several disk wind models first discussed in PSD I. These more physically accurate models show that PSD I's more approximate method was very robust. The PSD II calculations predict total mass loss rates and velocities marginally different from those published in PSD I. Additionally, PSD II find that models which display unsteady behavior in PSD I are also unsteady with the new method. The largest change caused by the new method is in the disk-wind opening angle: winds driven only by the disk radiation are more polar with the new method while winds driven by the disk and central object radiation are typically more equatorial.

In this paper, we will numerically check how strong, ordered magnetic fields can change disk winds driven by the line force for a given disk luminosity. We assume that the transport of angular momentum in the disk is dominated by local disk viscosity, for instance due to the local shear instability in weakly magnetized disk (Balbus & Hawley 1997). Instead of adding the magnetic fields to the PSD II model and solving consistently the equations of MHD, we simply start by adding some of the effects due to the magnetic fields, namely (1) the azimuthal force so the wind conserves the specific angular velocity along the streamlines and (2) the force perpendicular to the field lines so the geometry of the disk wind is controlled by the magnetic field. We thus adopt the popular concept that the magnetic field dominates outside the disk and at least near the disk surface, one can think of the magnetic field lines as rigid wires that control any flow (e.g., Blandford & Payne 1982; Pelletier & Pudritz 1992). Such an approach is clearly simplistic and can be applied only to sub-Alfvénic flows. Nevertheless, the results presented here provide a useful exploratory study of line-driven disk winds in the presence of a strong, large-scale field magnetic threading the disk.

The organization of the paper is as follows. In Section 2 we describe our numerical calculations; in Section 3 we present our results; in Section 4 we conclude with a brief discussion.

2. Method

To calculate the structure and evolution of a wind from a disk, we solve the equations of hydrodynamics

$$\frac{D\rho}{Dt} + \rho \nabla \cdot \mathbf{v} = 0, \quad (1)$$

$$\rho \frac{D\mathbf{v}}{Dt} = -\nabla(\rho c_s^2) + \rho \mathbf{g} + \rho \mathbf{F}^{rad} + \rho \mathbf{F}^{mc} \quad (2)$$

where ρ is the mass density, \mathbf{v} the velocity, \mathbf{g} the gravitational acceleration of the central object, \mathbf{F}^{rad} the total radiation force per unit mass, and \mathbf{F}^{mc} the total 'magnetocentrifugal' force. The term with \mathbf{F}^{mc} ensures that gas flows along an

assumed direction and conserves its specific angular velocity. The gas in the wind is isothermal with a sound speed c_s . We solve these equations in spherical polar coordinates (ρ, θ, ϕ) .

The geometry and assumptions needed to compute the radiation field from the disk and central object are as in PSD II (see also PSD I). The disk is flat, Keplerian, geometrically-thin and optically-thick. We specify the radiation field of the disk by assuming that the temperature follows the radial profile of the so-called α -disk (Shakura & Sunyaev 1973), and therefore depends only on the mass accretion rate in the disk, \dot{M}_a , and the mass and radius of the central object, M_* and r_* . In particular, the disk luminosity, $L_D \equiv GM_*\dot{M}_a/2r_*$. In models where the central object radiates, we take into account the stellar irradiation of the disk, assuming that the disk re-emits all absorbed energy locally and isotropically. We express the central object luminosity L_* in units of the disk luminosity $L_* = xL_D$. See PSD I and PSD II for further details.

Our numerical algorithm for evaluating the line force is described in PSD II. For a rotating flow, there may be an azimuthal component to the line force even in axisymmetry. However we set this component of the line force to zero because it is rather weak as compared to other components and is not of great importance (e.g., PSD II). Then we assume that the rotational velocity v_ϕ is determined by the azimuthal component of the magnetocentrifugal force. The description of our calculation of the 'magnetocentrifugal' force follows.

We choose the simplest geometry of the magnetic field and the flow: the poloidal component of the magnetic field, \mathbf{B}_p and of the velocity, \mathbf{v}_p are parallel to one another, and the inclination angle i between \mathbf{v}_p and the disk midplane is fixed for all locations and times. In other words, we constrain the geometry of the flow to straight cones of pre-specified, radius- and time-independent opening angle. In practice, we impose this geometry in the following way: (i) we evaluate the physical accelerations and the curvature terms in eq. 2, hereafter collectively referred to as

$$\mathbf{F}' = -\frac{1}{\rho}\nabla(\rho c_s^2) + \mathbf{g} + \mathbf{F}^{rad} + \mathbf{F}^i, \quad (3)$$

where \mathbf{F}^i represents the curvature terms appearing on the left hand side of eq. 2 when $\frac{D\mathbf{v}}{Dt}$ is expressed in the spherical polar coordinate system (e.g., Shu 1992):

$$\mathbf{F}^i = \begin{pmatrix} \frac{v_\theta^2 + v_\phi^2}{r} \\ \frac{v_\phi^2}{r} \cot \theta \\ 0 \end{pmatrix}, \quad (4)$$

(ii) we calculate the component of \mathbf{F}' perpendicular to a streamline:

$$\mathbf{F}'_\perp = \mathbf{\Lambda} \mathbf{F}', \quad (5)$$

where

$$\mathbf{\Lambda} = \begin{pmatrix} \sin^2(\theta - i) & \sin(\theta - i) \cos(\theta - i) & 0 \\ \sin(\theta - i) \cos(\theta - i) & \cos^2(\theta - i) & 0 \\ 0 & 0 & 0 \end{pmatrix}, \quad (6)$$

(iii) and finally we subtract \mathbf{F}'_\perp from \mathbf{F}' so the total remaining force is tangent to the streamline.

The disk outflow that conserves its specific angular velocity, $\Omega = v_\phi/(r \sin \theta)$ along a streamline is simply the flow that corotates with the disk, i.e., Ω is constant and equals to the disk rotational velocity, $\Omega_D = v_\phi(r_D, 90^\circ)/r_D$ at the footpoint of the streamline on the disk at the radius, r_D . To ensure corotation of the wind, we introduce the azimuthal force:

$$\mathbf{F}^t = \begin{pmatrix} 0 \\ 0 \\ 2 \frac{v_\phi(v_r \sin \theta + v_\theta \cos \theta)}{r \sin \theta} \end{pmatrix}. \quad (7)$$

Summarizing, our magnetocentrifugal force is

$$\mathbf{F}^{mc} = -\mathbf{\Lambda} \mathbf{F}' + \mathbf{F}^t. \quad (8)$$

As in PSD II, we use the ZEUS-2D code (Stone & Norman 1992) to numerically integrate the hydrodynamical equations (1) and (2). We did not change the transport step in the code and so the changes we made are just to the source step as outlined above.

We explore disk wind models for three cases: (I) a wind corotates with the disk ($\mathbf{F}'_{\perp} = 0$ and $F_{\phi}^t = 2v_{\phi}(v_r \sin \theta + v_{\theta} \cos \theta)/(r \sin \theta)$) ; (II) the wind geometry is fixed by adopting a fixed inclination angle between the poloidal component of the velocity and the disk midplane ($\mathbf{F}'_{\perp} = \Lambda \mathbf{F}'$ and $\mathbf{F}^t = 0$) ; and (III) a combination of (I) and (II) ($\mathbf{F}'_{\perp} = \Lambda \mathbf{F}'$ and $F_{\phi}^t = 2v_{\phi}(v_r \sin \theta + v_{\theta} \cos \theta)/(r \sin \theta)$).

In case I with $x = 0$, we decided to put an additional constraint on the radial velocity to produce outward flows. Near the disk midplane, fluctuations of the density and velocity can occur (e.g., PSD I). Additionally, the radial component of the radiation force is negative near the disk midplane and the central object (e.g., Icke 1980, PSD I). Thus v_r can be less than zero; gravity can dominate and pull the flow toward the center. To avoid this we apply the condition: $v_r = \max(v_r, -\cot \theta v_{\theta})$. This condition does not change the mass loss rate, but does reduce the wind opening angle.

To produce transonic flows in cases II and III, we need to increase the density along the disk midplane, ρ_o , from $10^{-9} \text{ g cm}^{-3}$ (as used by PSD I) up to $10^{-4} \text{ g cm}^{-3}$. For low ρ_o , the wind velocity does not depend on ρ , the mass loss rate is proportional to ρ_o and may be higher than the mass accretion rate. For $\rho_o \gtrsim 10^{-4} \text{ g cm}^{-3}$ the mass loss rate is dramatically lower, does not change with ρ_o , and the flow is subsonic near the disk midplane. These are desired properties of the outflow; we expect gas near the midplane to be nearly in hydrostatic equilibrium. Equally important, we assume that the disk is in a steady state so the mass loss rate should be lower than the mass accretion rate.

In reality, gas near the disk midplane (inside the disk) is in hydrostatic equilibrium for the densities lower than those we assumed because the radiation force is lower as the radiation becomes isotropic. We would like to stress that we treat the region very close to the midplane as a boundary condition and do not attempt to model the disk interior.

As in PSD I and PSD II, we calculate disk winds with model parameters suitable for a typical nMCV (see PSD I's Table 1 and our Table 1). We vary the disk and central object luminosity and the inclination angle. We hold all other parameters fixed, in particular the parameters of the CAK force multiplier: $k = 0.2$, $\alpha = 0.6$ and $M_{max} = 4400$ (see PSD I). Nevertheless we can use our results to predict the wind properties for other parameters and systems – such as AGN – by applying the dimensionless form of the hydrodynamic equations and the scaling formulae as discussed in PSD I and Proga (1999).

3. Results

PSD I and PSD II showed that radiation-driven winds from a disk fall into two categories: 1) intrinsically unsteady with large fluctuations in density and velocity, and 2) steady with smooth density and velocity. The type of the flow is set by the geometry of the radiation field, parametrized by x : if the radiation field is dominated by the disk ($x < 1$) then the flow is unsteady, and if the radiation is dominated by the central object ($x \gtrsim 1$) then the flow is steady. The geometry of the radiation field also determines the geometry of the flow; the wind becomes more polar as x decreases. However the mass-loss rate and terminal velocity are insensitive to geometry and depend more on the total system luminosity, $L_D + L_*$. We recalculated some of the PSD II models to check how inclusion of the magnetocentrifugal force will change line-driven disk winds.

Figure 1 compares the density in the wind in two models from PSD II where they used a generalized CAK method (top panels), models using PSD II's method but conserving specific angular velocity – our case I (middle panels), and models using PSD II's method, conserving specific angular velocity and having fixed inclination angle of the stream lines – our case III (bottom panels). Models in case III (bottom panels) are with the inclination angles approximately equal to those in the PSD II case (the top panels). The left column shows the results for a model with $\dot{M}_a = 10^{-8} \text{ M}_{\odot} \text{ yr}^{-1}$ and $x = 0$, while the right column shows the results with $\dot{M}_a = \pi \times 10^{-8} \text{ M}_{\odot} \text{ yr}^{-1}$ and $x = 1$. The former corresponds to the fiducial $x = 0$ model while the latter corresponds to the fiducial $x = 1$ model discussed in detail in PSD I and PSD II.

We start with describing the $x = 0$ wind model (left column panels). The most striking yet expected difference between PSD II's case (top) and our case I (middle) is a decrease of the wind opening angle, ω from 50° to 15° when the specific angular momentum conservation is replaced by the specific angular velocity conservation. This result is caused by a much stronger centrifugal force in our case I than in the PSD II case which is also reflected in an increase of the radial velocity by more than one order of magnitude (Table 1). Another big difference between the two cases is in the mass loss rate, \dot{M}_w which increases from $5.5 \times 10^{-14} \text{ M}_{\odot} \text{ yr}^{-1}$ to $1.3 \times 10^{-12} \text{ M}_{\odot} \text{ yr}^{-1}$. An unchanged property in these two cases is that the wind is unsteady. The quantitative changes between PSD I's case (top) and case III (bottom) are similar or smaller than the changes described above (see Table 1). The most pronounced change caused by holding the inclination angle fixed is that the wind becomes steady. However this is not surprising because models with the fixed, rigid geometry are pseudo one-dimensional and the flow has one degree of freedom in space. In PSD I and PSD II models where the wind geometry is calculated self-consistently, a strong radial radiation force is required to produce a steady outflow.

The $x=1$ wind model (top right hand panel of Figure 1) is an example of a steady outflow from PSD II. This model remains steady in the two other cases shown in the figure and in case I listed in Table 1 (run Ic). The model changes from case to case mainly in the radial and rotational velocities which increase when the azimuthal force is added (middle and bottom panel). For example, the radial velocity increased from 3500 km s^{-1} in PSD II's run C (top panel) to 28000 km s^{-1} in our run IIIc (bottom panel). As in the $x=0$ wind model, adding the azimuthal force also reduces the wind opening angle (middle panel). However an increase in the mass loss rate from PSD II's case (top panel) to our case II (bottom panel) is only a factor of ~ 2 . The mass loss rate is practically the same in case II and case III (run IIc and IIIc).

Models presented in Figure 1 both for $x = 0$ and $x = 1$ suggest that an increase in the mass loss rate due to conservation of the specific angular velocity decreases with the disk luminosity. Our other results, shown in Table 1, confirm this. For example, the $x=0$ model Ib with $\dot{M}_a = \pi \times 10^{-8} \text{ M}_\odot \text{ yr}^{-1}$ has \dot{M}_w higher than the corresponding PSD II's model B by a factor of ~ 3 while an increase of \dot{M}_w for models with $\dot{M}_a = 10^{-8} \text{ M}_\odot \text{ yr}^{-1}$ is by a factor ~ 24 (i.e., runs A and Ia).

The mass loss rate of the line-driven disk wind also increases by imposing the wind geometry such that $i > 0^\circ$ as comparison of our results in case II and from PSD II reveals. Once the geometry is fixed the mass loss rate does not change with adding the azimuthal force – the corresponding models in our case II and III have the same \dot{M}_w .

Purely line-driven $x=0$ winds have streamlines perpendicular to the disk midplane near the midplane because the total horizontal force is negligible in comparison with the vertical force due to lines. This property of disk winds has been assumed in analytic studies of line-driven disk winds (e.g., Vitello & Shlosman 1988). We calculated a model assuming $i = 0^\circ$ (run IIa) and find that the mass loss rate is very similar to the corresponding PSD II's run A. This confirms then that the mass loss rate in line-driven disk winds for $x = 0$ is determined in the regions where the matter flows still perpendicularly to the disk.

4. Conclusions and Discussion

We have studied winds from accretion disks with very strong organized magnetic fields and the radiation force due to lines. We use numerical methods to solve the two-dimensional, time-dependent equations of hydrodynamics. We have accounted for the radiation force using a generalized multidimensional formulation of the Sobolev approximation. To include the effects of the strong magnetic field we have added to the hydrodynamic equation an approximate magnetocentrifugal force. Our approach of treating the latter allows us to study cases where the wind geometry is controlled entirely by the magnetic field with the lines of the poloidal component of the field, \mathbf{B}_p being straight and inclined at a fixed angle to the disk midplane where the specific angular velocity is conserved along the streamlines due to the magnetic azimuthal force, or both.

Our simulations of line-driven disk winds show that inclusion of the azimuthal force, \mathbf{F}^t which makes the wind corotate with the disk, increases the wind mass loss rate significantly only for low disk luminosities. As expected such winds have much higher velocities than winds with zero azimuthal force. Fixing the wind geometry effectively reduces the flow from two-dimensional to one-dimensional. This in turn stabilizes winds which are unsteady when the geometry is allowed to be determined self-consistently. The inclination angle between the poloidal velocity and the normal to the disk midplane is important. If it is higher than zero it can significantly increase the mass loss rate for low luminosities, and increase the wind velocity for all luminosities. The presence of the azimuthal force does not change the mass loss rate if the geometry is fixed.

It is very intriguing that the mass loss rate can be enhanced by the magnetocentrifugal force the most for low luminosities where line force is weak and at the same time the mass loss rate remains a strong function of the disk luminosity for all luminosities. In particular, there is no wind when $\dot{M}_a \lesssim 10^{-8} \text{ M}_\odot \text{ yr}^{-1}$ as in purely line-driven case (e.g., PSD I; Proga 1999).

Model IIa' with $i = 0$ is steady and has the same \dot{M}_w as the corresponding PSD II model. The mass loss rate is then the same regardless of the time behavior. This is consistent with PSD I conclusion that the mass loss rate depends predominately on the total system luminosity.

Drew & Proga (1999) applied results from PSD I, PSD II and Proga 1999 to nMCV. In particular, they compared mass loss rates predicted by the models with observational constraints. They concluded that either mass accretion rates in high-state nMCV are higher than presently thought by a factor of 2-3 or that radiation pressure alone is not quite sufficient to drive the observed hypersonic flows. If the latter were true then an obvious candidate to assist radiation pressure in these cases is MHD (e.g., Drew & Proga 1999).

An increase of the mass loss rate due to inclusion of a magnetocentrifugal force (our case I) brings our predictions close to the observational estimates for nMCVs. However we should bear in mind that at the same time, the radial velocity of

the wind increases above the observed velocities in nMCVs that are of the order a few thousand km s^{-1} . The increase of the wind velocity may not be large if the magnetic field is moderately strong and spins up the disk wind only close to its base where the mass loss rate is determined. Then farther away from the disk the wind would gain less or no angular momentum and velocities would be similar to those in the case without the magnetic field at all.

Outflows which conserve specific angular velocity have a higher rotational velocity than those which conserve specific angular momentum. The former also have higher terminal velocities due to stronger centrifugal force. Additionally in the wind where the specific angular velocity is conserved the rotational velocity is comparable to the terminal velocity while in the wind where the specific angular momentum is conserved the rotational velocity decreases asymptotically to zero with increasing radius and is therefore much lower than the terminal velocity. Thus we should be able to distinguish these two kinds of winds based on their line profiles. For example, highly rotating winds should produce emission lines much broader than slowly rotating, expanding winds, if we see the disk edge-on.

So far we have discussed changes of the line-driven wind caused by inclusion of the magnetocentrifugal force. However we can also anticipate some changes in the magnetocentrifugal wind if we add the line force. For example, there may be a difference in the wind collimation caused by the line force. The centrifugal force decollimates the magnetocentrifugal outflow near the disk as i must be greater than 30° . In such a case the magnetic field collimates the outflow only beyond the Alfvén surface where the pinch force exerted by the toroidal component of the field operates. In the case with a significant line driving, the magnetic field does not have to be inclined at the angle $> 30^\circ$. Then in such case, outflows are more collimated than pure magnetocentrifugal outflows from the start and may end up more collimated far away from the disk.

Let us now discuss some results of other related works. Recently Ogilvie & Livio (1998) studied a thin accretion disk threaded by a poloidal magnetic field. Their purpose was to determine qualitatively how much thermal assistance is required for the flow to pass through the slow magnetosonic surface. They found that a certain potential difference must be overcome even when $i > 30^\circ$ and that thermal energy is not sufficient to launch an outflow from a magnetized disk. Ogilvie & Livio suggested that an additional source of energy, such as coronal heating may be required. PSD I showed the radiative line force can drive disk winds. Thus the ‘missing’ energy may be in the radiation field. Our calculations here show that if the disk luminosity is sufficiently high the line and magnetocentrifugal forces produce strong transonic winds regardless of the wind geometry. Then the magnetocentrifugal force can assist the line force in producing disk winds – our approach to the problem or the line force or/and the thermal force can well assist MHD – Ogilvie & Livio’s approach (see also Wardle & Königl 1993; Cao & Spruit 1994, for instance). In seeking a steady state solution of a line-driven disk wind, Vitello & Shlosman (1988) also found that the flow must overcome a potential difference – an increase of the vertical gravity component with height. They suggested that for the radiation force to increase with height above the disk midplane and overcome this potential difference a very particular variation in the ionization state of the gas is required.

There are a number of limitations of our treatment of magnetic fields which are worthy of mention.

Our models do not include the whole richness of MHD because we approximate the Lorentz force by the ‘magnetocentrifugal’ force (eqs 3-8) instead of solving self-consistently the equation of motion and the induction equation. We have included effects of a magnetic field on the disk winds in a simplistic manner that mimics some effects of a very strong, organized magnetic field where $B_\phi \lesssim B_p$ near the disk surface. The magnetic field is treated as a rigid wire that controls the flow geometry outside the disk. More quantitatively, this corresponds to the situation where outside the disk, at least near the disk photosphere, the magnetic field dominates i.e., the magnetic pressure exceeds the disk gas pressure $\beta \equiv 8\pi p_D/B_D^2 < 1$. Inside the disk however the situation may be different. We assume that the disk is in a steady state that is also stable. In such a case, the regions near the disk midplane are likely supported by the gas pressure and the magnetic pressure should be smaller than the gas pressure, i.e., $\beta \gtrsim 1$, otherwise the disk may be unstable (Stella & Rosner 1984). Using the system parameters adopted here: $c_s = 14 \text{ km s}^{-1}$ and $\rho_o = 10^{-4} \text{ g cm}^{-3}$, we find that the $\beta \gtrsim 1$ condition yields a maximum value for the disk magnetic fields strength of the order of $\sim 10^5 \text{ G}$. Our assumption that poloidal magnetic field lines are straight excludes any magnetic tension in the (r, θ) plane.

In our cases I and III we assume that the specific angular velocity, Ω is conserved along a streamline from the footpoint of the line to infinity or rather to the outer boundary of the computational domain. However in a steady state axisymmetric MHD flow, the quantity which is conserved is the total angular momentum per unit mass which can be written as

$$l = \Omega r^2 \sin^2 \theta - \frac{r \sin \theta B_\phi}{4\pi\kappa} \equiv \Omega_D r_A^2, \quad (9)$$

where r_A is the position of the the Alfvén point of the flow on the streamline, and $\kappa = \rho v_p/B_p$ is the mass load– another constant along the streamline (e.g., Pelletier & Pudritz 1992). The total angular momentum has contributions from both the flowing rotating gas and the twisted magnetic field. This means that as the material angular momentum, $\Omega r^2 \sin^2 \theta$

increases due to corotation with the disk, the toroidal component of the magnetic field must increase so the total angular momentum is conserved. Then our approximation in cases I and III corresponds to the situation where near the disk the total angular momentum is dominated by the contribution from the twisted magnetic field and the Alfvénic surface is beyond our computational domain. In other words our approximation is valid in the region where the outflow is sub-Alfvénic. Consequently, our approach does not allow us to study collimation of the wind by the magnetic field because this happens beyond the fast magnetosonic surface where the flow is super-Alfvénic.

PSD II's models and ours in case II correspond to the other extreme case where the total angular momentum has no contribution from the twisted magnetic field and the material angular momentum is conserved.

Our treatment of magnetic fields does not include effects of the magnetic pressure. The magnetocentrifugal driving presupposes the existence of a strong poloidal magnetic field comparable to the toroidal magnetic field near the disk surface, $|B_\phi/B_p| \lesssim 1$. However when the poloidal magnetic field is weaker than the toroidal magnetic field, $|B_\phi/B_p| \gg 1$ the magnetic pressure may be dynamically important in driving disk winds (e.g., Uchida & Shibata 1985; Pudritz & Norman 1986, Shibata & Uchida 1986, Contopoulos 1995; Kudoh & Shibata 1997; Ouyed & Pudritz 1997 and references therein). For $|B_\phi/B_p| \gg 1$, there is initially the buildup of the toroidal magnetic field by the differential rotation of the disk that in turn generates the magnetic pressure of the toroidal field. The magnetic pressure then gives rise to a self-starting wind. To produce a steady outflow driven by the magnetic pressure a steady supply of the advected toroidal magnetic flux at the wind base is needed, otherwise the outflow is likely a transient (e.g., Königl 1993, Contopoulos 1995, Ouyed & Pudritz 1997). However it is not clear whether the differential rotation of the disk can produce such a supply of the toroidal magnetic flux to match the escape of magnetic flux in the wind and even if it does whether such a system will be stable (e.g., Contopoulos 1995, Ouyed & Pudritz 1997 and references therein).

Concluding, we would like to stress that a further development of models of radiation-driven winds from disks should include taking into account magnetic field but it is equally important to consider adding the radiation force to models of MHD winds from luminous disks. Both kinds of models are quite well understood now and if merged they could allow us to study better disk winds in systems such as cataclysmic variables and AGNs. As we mentioned above thermal assistance may not be sufficient to launch wind from a magnetized disk and we should consider not only coronal heating but also line driving.

ACKNOWLEDGEMENTS: We thank John Cannizzo, Janet Drew, Achim Feldmeier, Tim Kallman, Scott Kenyon, Mario Livio, and James Stone for comments on earlier drafts of this paper. We also thank Steven Shore and an anonymous referee for comments that helped us clarify our presentation. This work was performed while the author held a National Research Council Research Associateship at NASA/GSFC. Computations were supported by NASA grant NRA-97-12-055-154.

REFERENCES

- Balbus, S.A., & Hawley, J.F. 1998, *Rev. Mod. Phys.*, 70, 1
- Begelman M.C., McKee C.F., Shields G. A. 1983, *ApJ*, 271, 70
- Blandford R.D., Payne D.G. 1982, *MNRAS*, 199, 883
- Bogovalov S.V. 1997, *A&A*, 323, 634
- Cannizzo J. K., Pudritz R.E. 1988, *ApJ*, 327, 840
- Cao X., Spruit H.C. 1994, *A&A*, 287, 80
- Castor J.I., Abbott D.C., Klein R.I. 1975, *ApJ*, 195, 157 (CAK)
- Contopoulos J. 1995, *ApJ*, 450, 616
- Drew J.E., Proga D., in “*Cataclysmic Variables*”, *Symposium in Honour of Brian Warner*, Oxford 1999, ed. by P. Charles, A. King, D. O’Donoghue, in press
- Friend D.B., Abbott D.C., 1986 *ApJ*, 311, 701
- Icke V. 1980, *AJ*, 85, 329
- Königl A. 1993, in “*Astrophysical Jets*”, ed. by D.P. O’Dea (Cambridge: Cambridge Univ. Press), 239
- Krasnopolsky R., Li Z.-Y., Blandford R., 1999, *ApJ*, 526, 631
- Kudoh T., Shibata K. 1997, *ApJ*, 474, 362
- Murray N., Chiang J., Grossman S.A., Voit G.M. 1995, *ApJ*, 451, 498
- Ogilvie G.I., Livio M. 1998, *ApJ*, 499, 329
- Ouyed R., Pudritz R.E. 1997, *ApJ*, 484, 794
- Owocki S.P., Cranmer S.R., Gayley K.G. 1996, *ApJ*, 472, L115
- Pauldrach A., Puls J., Kudritzki R.P. 1986, *A&A*, 164, 86
- Pelletier G., Pudritz R.E. 1992, *ApJ*, 394, 117
- Pereyra N.A., Kallman T.R. Blondin J.M. 1997, *ApJ*, 477, 368
- Proga D. 1999, *MNRAS*, 304, 938
- Proga D., Stone J.M., Drew J.E. 1998, *MNRAS*, 295, 595 (PSD I)
- Proga D., Stone J.M., Drew J.E. 1999, *MNRAS*, 310, 476 (PSD II)
- Pudritz R.E., Norman C.A. 1986, *ApJ*, 301, 571
- Shakura N.I., Sunyaev R.A. 1973 *A&A*, 24, 337
- Shibata K., Uchida Y. 1986, *PASJ*, 38, 631
- Shu, F. 1992, *The Physics of Astrophysics*, Vol. 2, Gas dynamics (Mill Valley: University Science Books)
- Stellar L., Rosner R. 1984, *ApJ*, 277, 312
- Stone J.M., Norman M.L. 1994, *ApJ*, 433, 746
- Uchida Y., Shibata K. 1985, *PASJ*, 37, 515
- Ustyugova G.V., Koldoba A.V., Romanova M.M. Chechetkin V.M. Lovelace R.V.E. 1999, *ApJ*, 516, 221
- Vitello P.A.J., Shlosman I., 1988 *ApJ*, 327, 680
- Wardle M., Königl A. 1993, *ApJ*, 410, 218
- Woods, D. T., Klein, R. I., Castor, J. I., McKee, C. F., Bell, J. B. 1996, *ApJ*, 461, 767

Table 1. Summary of results for disc winds

run	\dot{M}_a ($M_\odot \text{ yr}^{-1}$)	x	\dot{M}_w ($M_\odot \text{ yr}^{-1}$)	$v_r(10r_*)$ (km s^{-1})	ω or $(90^\circ - i)^*$ degrees
PSD II					
A	10^{-8}	0	5.5×10^{-14}	900	50
B	$\pi \times 10^{-8}$	0	4.0×10^{-12}	3500	60
C	$\pi \times 10^{-8}$	1	2.1×10^{-11}	3500	32
I					
a	10^{-8}	0	1.3×10^{-12}	15000	15
b	$\pi \times 10^{-8}$	0	1.3×10^{-11}	20000	38
c	$\pi \times 10^{-8}$	1	2.4×10^{-11}	32000	12
II					
a	10^{-8}	0	6.3×10^{-14}	600	90^\dagger
a'	10^{-8}	0	6.3×10^{-13}	1100	60^\dagger
c	$\pi \times 10^{-8}$	1	4.2×10^{-11}	5000	30^\dagger
III					
a	10^{-8}	0	6.3×10^{-13}	16000	60^\dagger
c	$\pi \times 10^{-8}$	1	4.2×10^{-11}	28000	30^\dagger

* For all models from PSD II and our models in case I, the last column lists the wind opening angle, ω . While for models in cases II and III, the last column lists $90^\circ - i$ (marked with \dagger), where i is the assumed inclination angle between the poloidal component of the velocity and the normal to the disk midplane; note that then $\omega \approx (90^\circ - i)$.

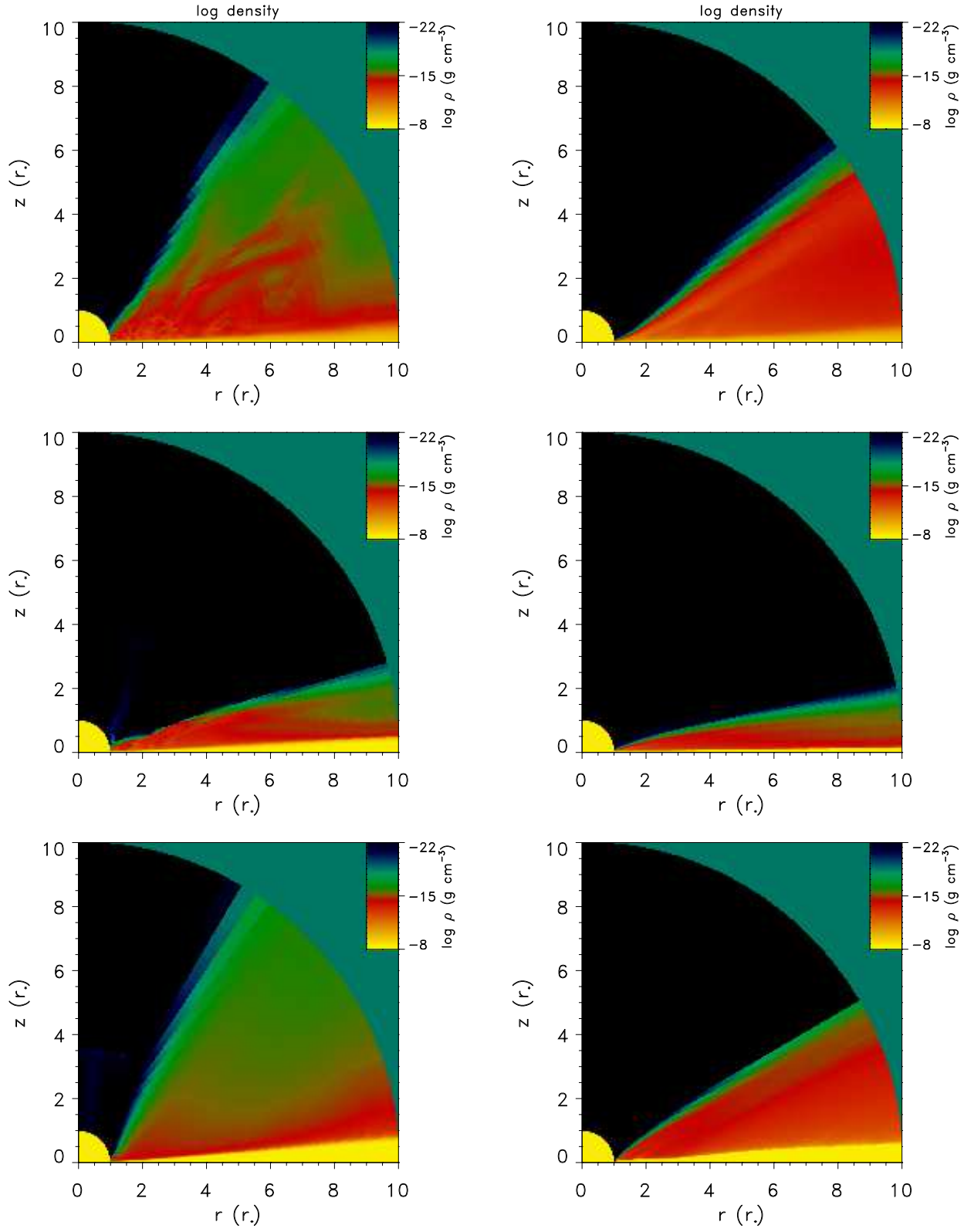


Fig. 1.— The color density maps in two models computed using the method of PSD II (top panels), the PSD II method with the specific angular velocity conservation (middle panels), and the latter with a fixed inclination angle of streamlines (bottom panels). The left column shows the results for the $x = 0$ model while the right column shows results for the $x = 1$ model (see table 2, and section 3.1 for discussion).

This figure "f1Lb.jpg" is available in "jpg" format from:

<http://arxiv.org/ps/astro-ph/0002441v1>

This figure "f1Lm.jpg" is available in "jpg" format from:

<http://arxiv.org/ps/astro-ph/0002441v1>

This figure "f1Lt.jpg" is available in "jpg" format from:

<http://arxiv.org/ps/astro-ph/0002441v1>

This figure "f1Rb.jpg" is available in "jpg" format from:

<http://arxiv.org/ps/astro-ph/0002441v1>

This figure "f1Rm.jpg" is available in "jpg" format from:

<http://arxiv.org/ps/astro-ph/0002441v1>

This figure "f1Rt.jpg" is available in "jpg" format from:

<http://arxiv.org/ps/astro-ph/0002441v1>